Supporting Information

Launching Directional Hypersonic Surface Waves in A Monolithic Gallium Phosphide Nanodisk: Two Holes Are Better Than One

Yongxian Yan,[1,3,†] Tao Zhu,[1,†] Qiancheng Zhao,[1,4] Rodrigo Berté,[2,] and Yi Li[1,*]*

1. School of Microelectronics, MOE Engineering Research Center of Integrated Circuits for Next Generation Communications, Southern University of Science and Technology, Shenzhen 518055, Guangdong, China

2. Instituto de Física da Universidade Federal de Goiás, 74001-970 Goiânia-GO, Brazil

3. Department of Applied Physics, The Hong Kong Polytechnic University, Hong Kong, China.

4. Wuhan National Laboratory for Optoelectronics (WNLO), Wuhan, China

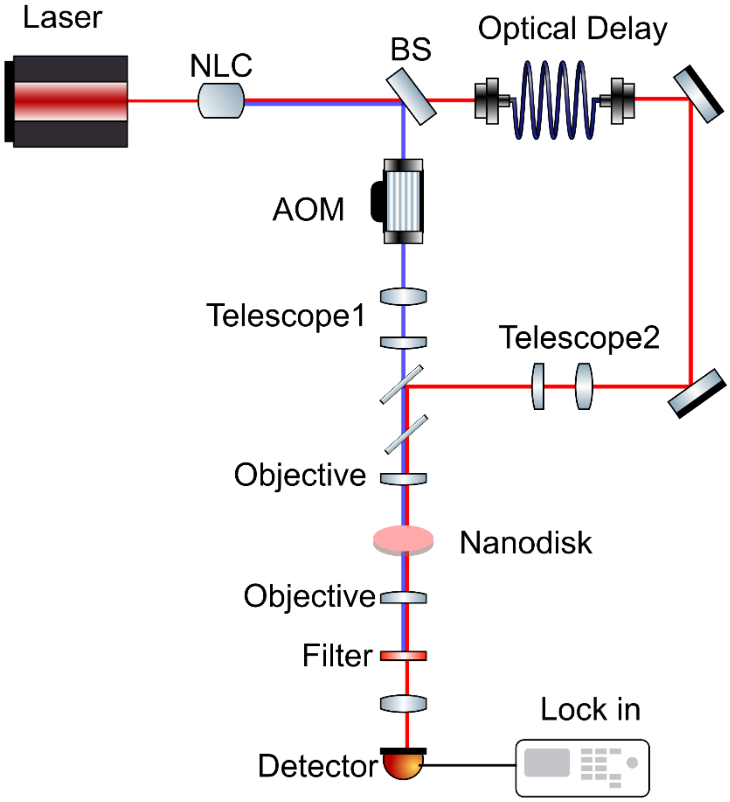

Figure S1. Optical set-up that excites and detects SAWs. A laser beam from Ti-Sapphire optical parametric oscillator (OPO) at 800 nm wavelength enters a nonlinear crystal (NLC), yielding its second harmonic at a 400 nm, used as a pump beam, as well as part of the original 800 nm, used as the probe. After a beam splitter (BS), the 400 nm one passes through an acoustic optical modulator (AOM), while the other goes into the delay line. Then the beams are focused on the nanodisk device using two separate telescope systems. The transmitted light at 800 nm will be analyzed with photodetectors and an electronic lock-in system.

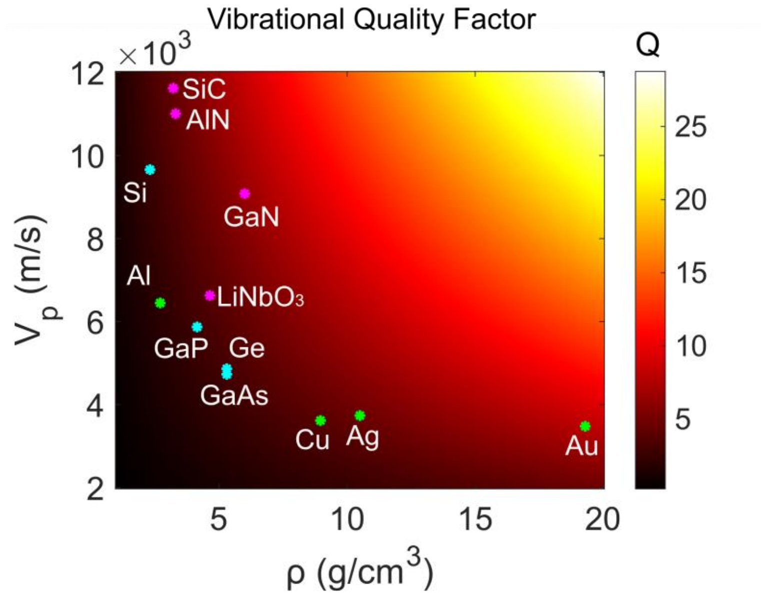

Figure S2. The quality factor of photoacoustic response Q as a function of material density $\boldsymbol{\rho}$ and pressure wave velocity $\boldsymbol{V_p}$. In Figure, the quality factors of these materials are displayed in a map where the density $\boldsymbol{\rho}$ and the velocity of pressure wave $\boldsymbol{c_p}$ have arbitrary values. We can see that the difference between metals and dielectrics is trivial here. There is also plenty of space on the top right corner where novel materials are encouraged to come out with both large $\boldsymbol{\rho}$ and $\boldsymbol{V_p}$.

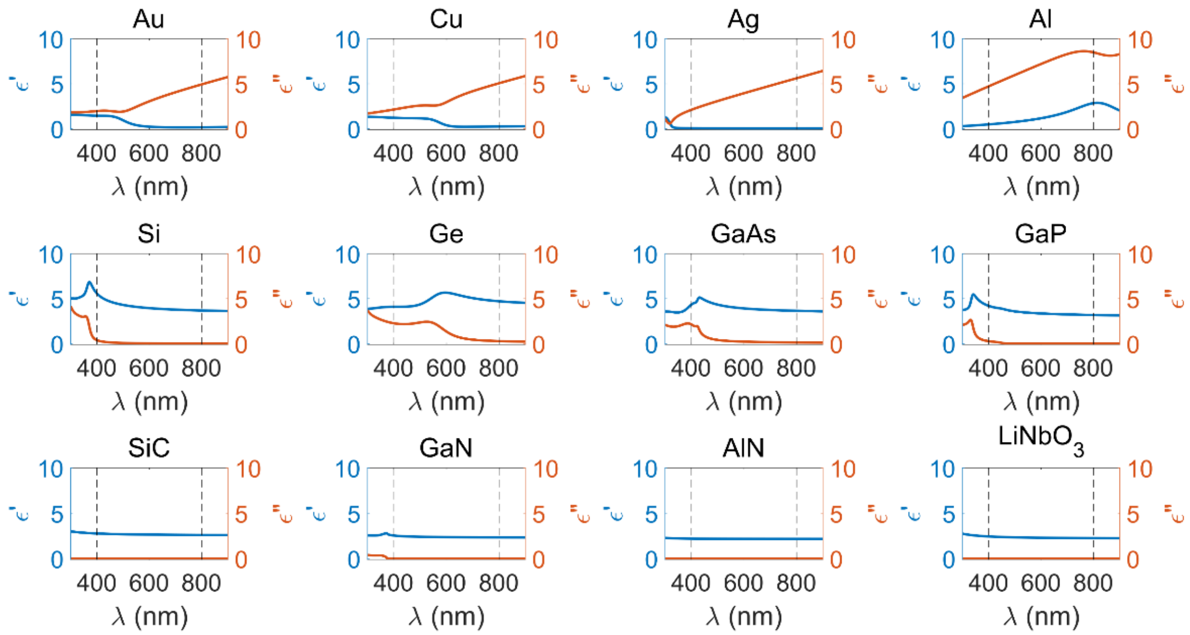

Figure S3. Relative Permittivity (both real and imaginary parts) of 12 material candidates

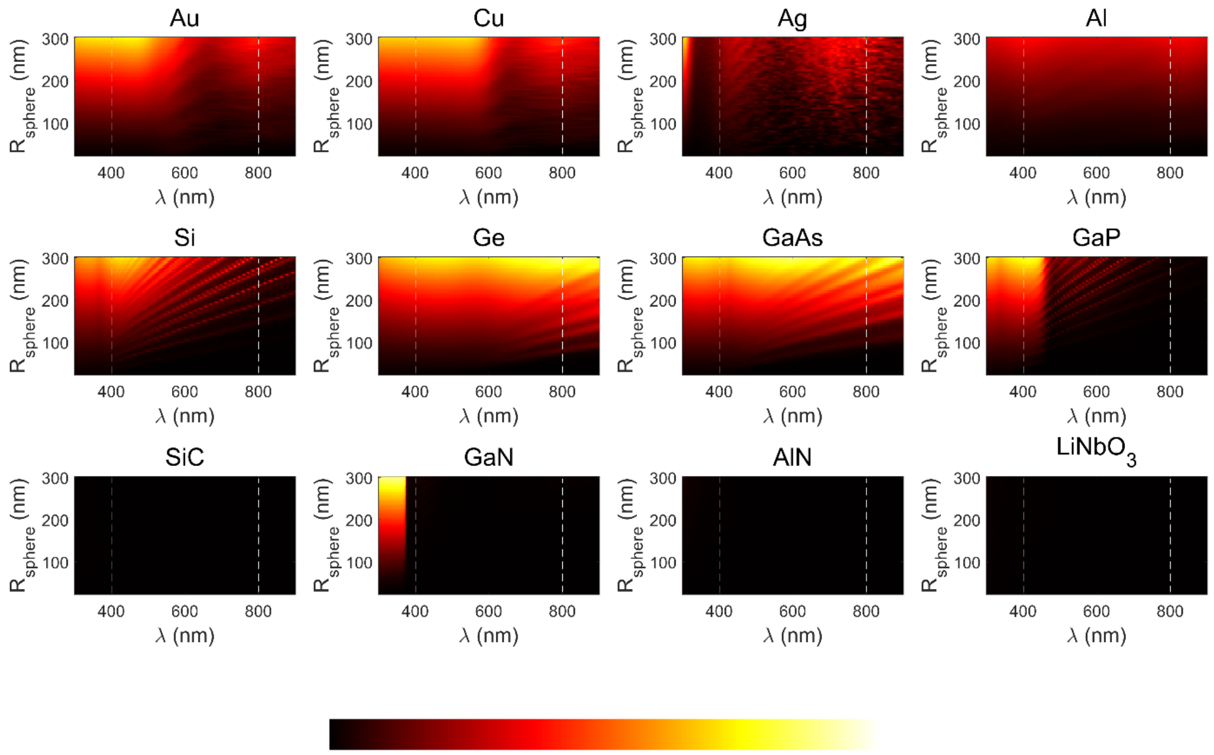

Figure S4. Absorption cross-sections of 12 material candidates. Dashed lines point out the position of 400 nm and 800 nm.

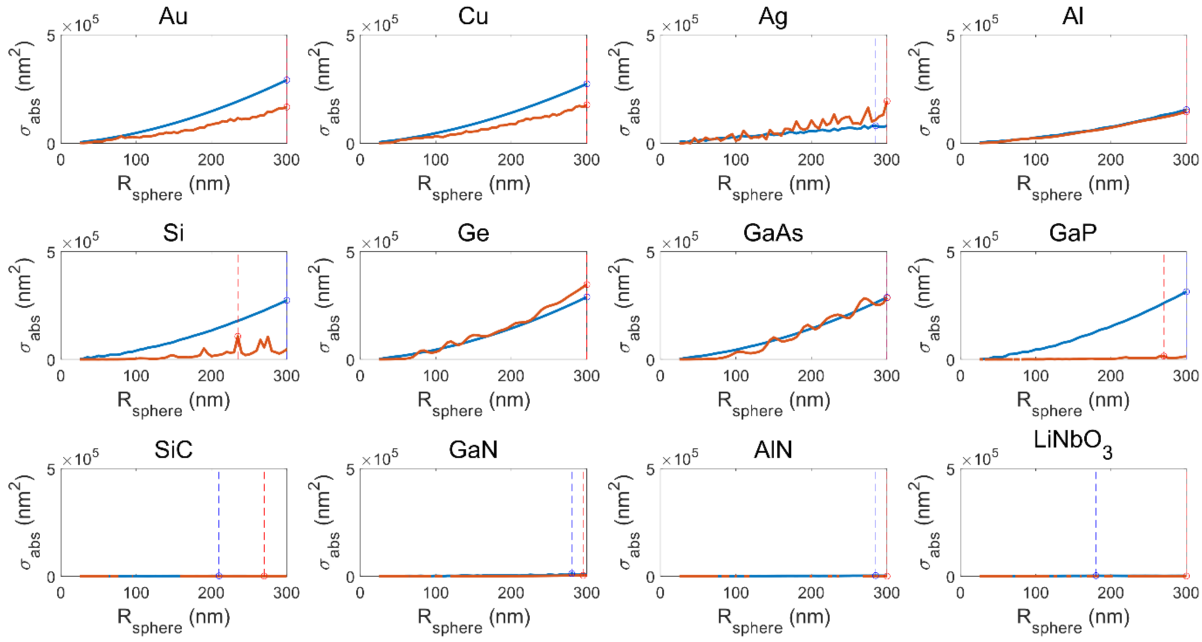

Figure S5. Absorption cross-sections of 12 material candidates at 400 nm (blue) and 800 nm (red) wavelength as a function of sphere radius.

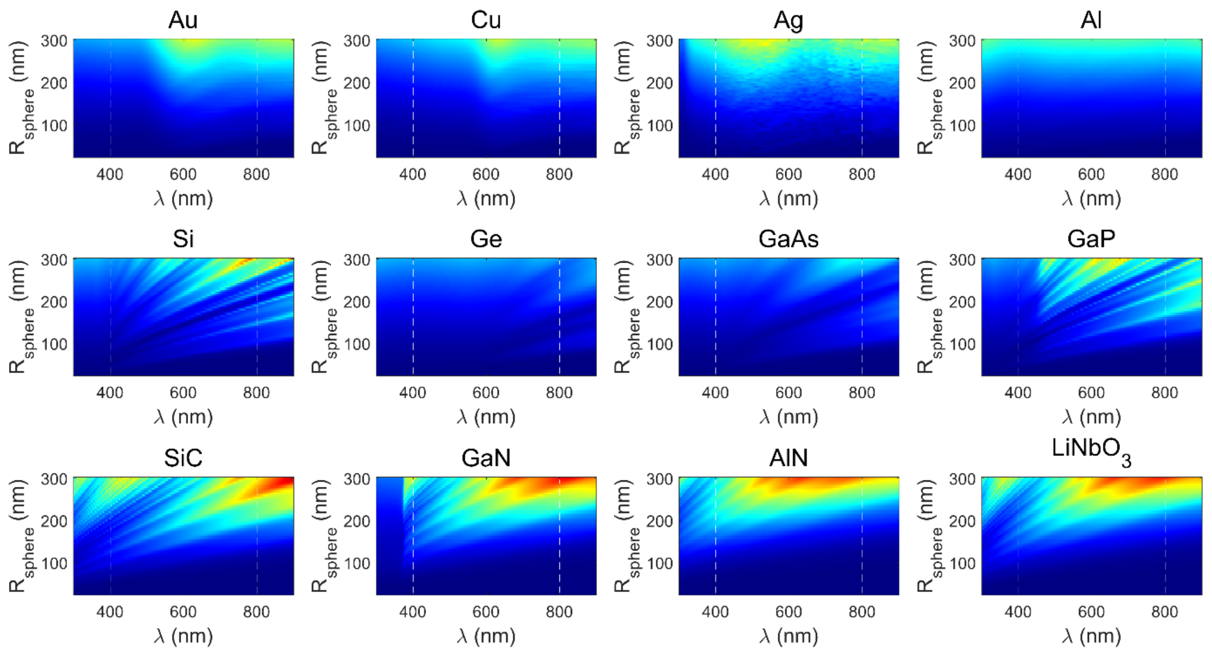

Figure S6. Scattering cross-sections of 12 material candidates.

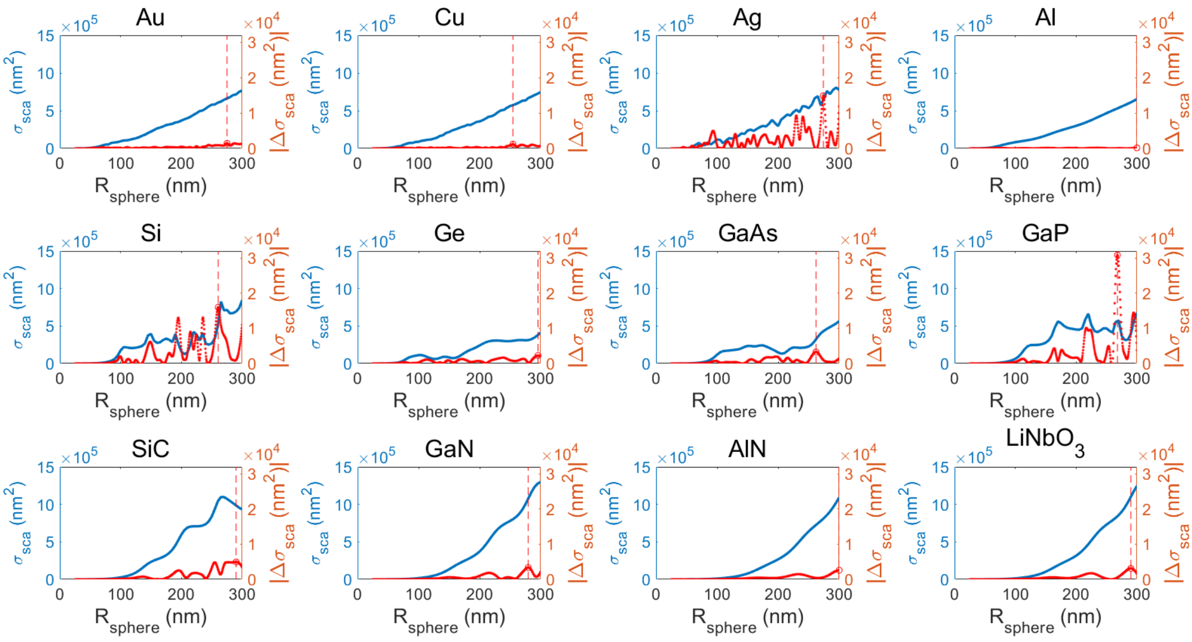

Figure S7. Scattering cross-sections and the deviation of scattering cross-sections of 12 material candidates at 800 nm wavelength as a function of sphere radius.

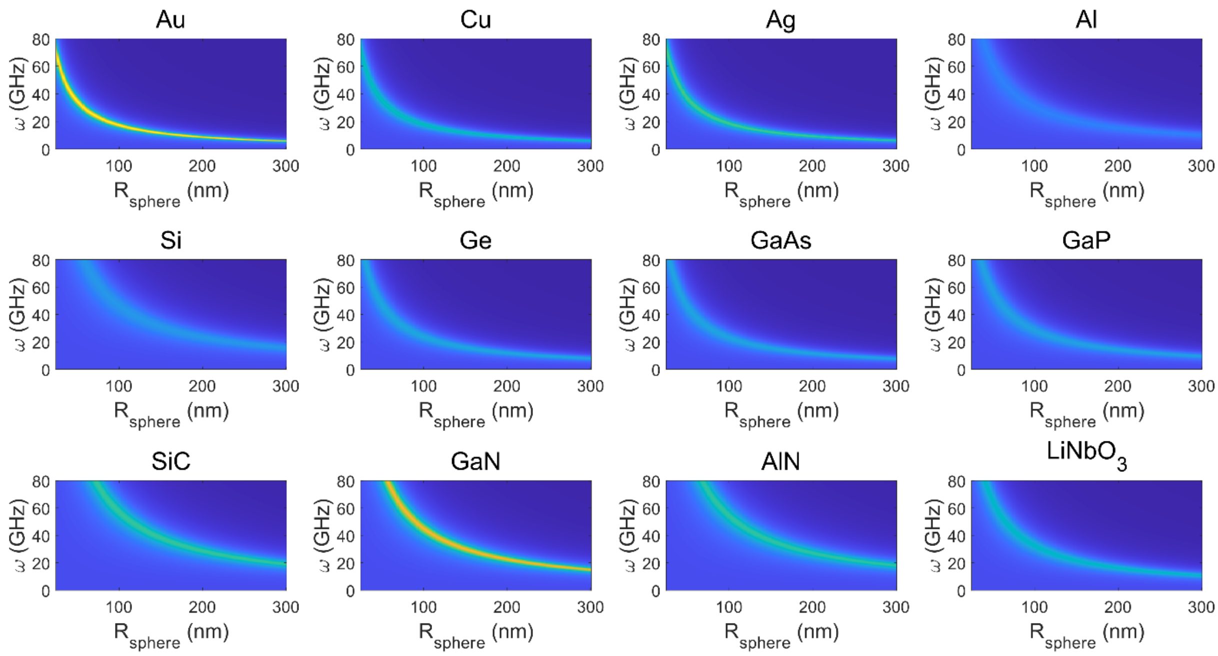

Figure S8. Acoustic radial displacement of 12 material candidates

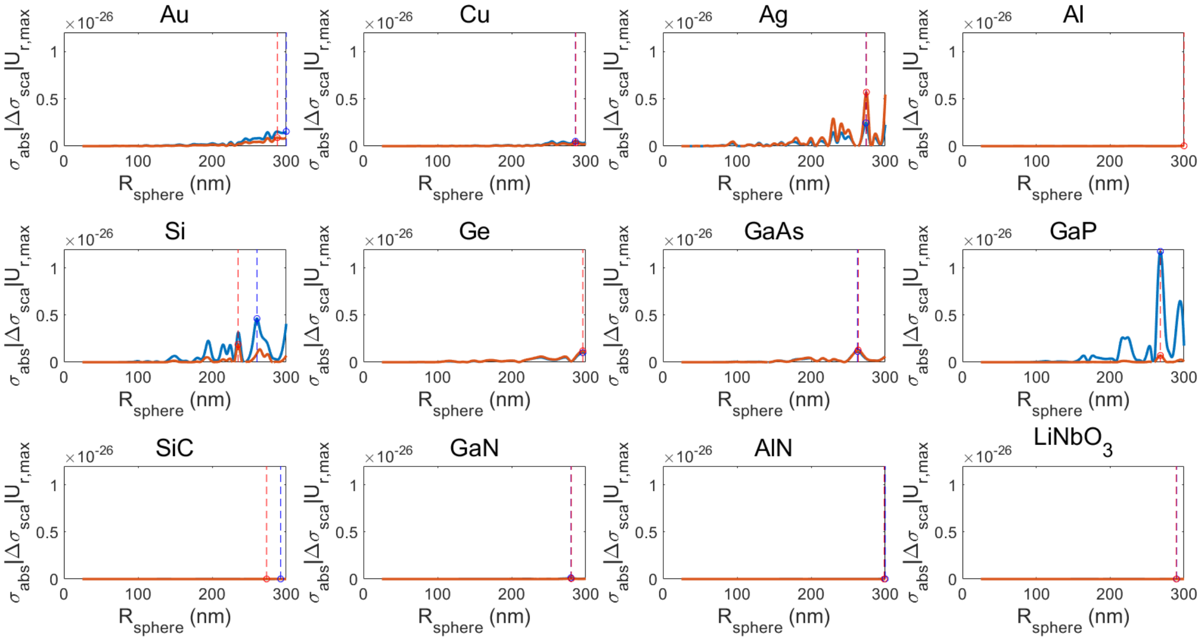

Figure S9. Figure of merit (FOM) of 12 material candidates

Table S1. The radii of the materials when the maximum FOM is achieved. (Unit: nm)

	SiC	**LiNbO₃**	**AlN**	**Al**	**GaN**	**Cu**	**Ge**	**GaAs**	**Au**	**Ag**	**Si**	**GaP**
400 nm – 800 nm	290	290	>300	>300	280	285	295	260	>300	275	260	**270**
800 nm – 800 nm	270	290	>300	>300	280	285	295	265	290	**275**	235	270

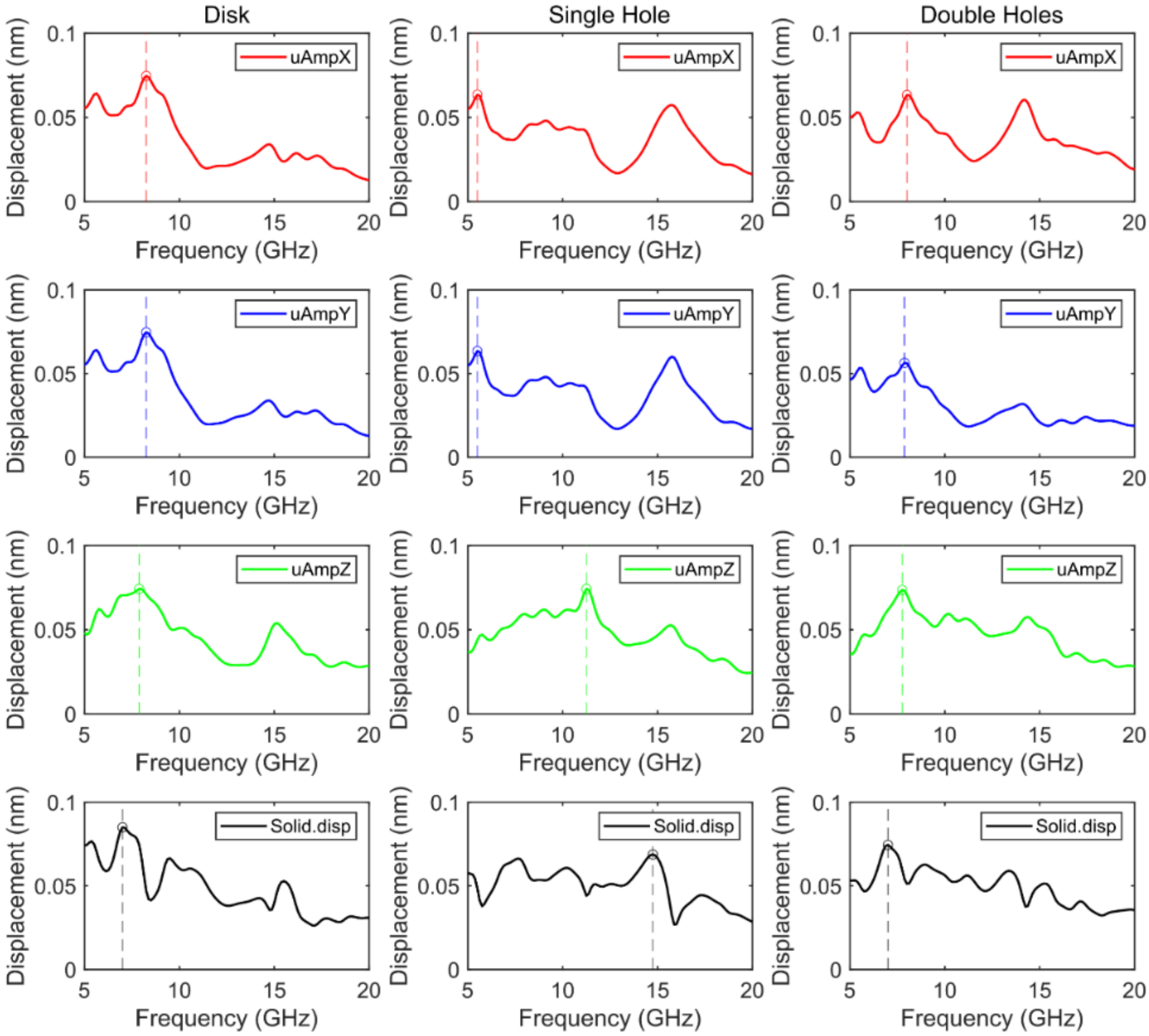

Figure S10. X, Y, Z and total displacements of three types of GaP nanodisks corresponding to Figure 2.

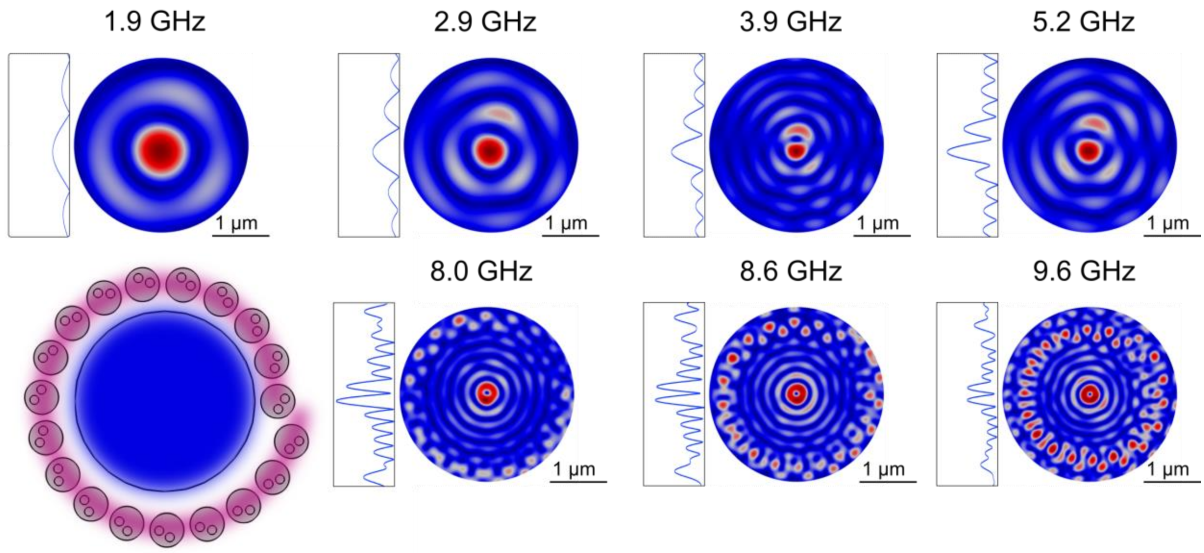

Figure S11. Top view and normalized vibration patterns at different resonant frequencies. The 1D blue-curves display the radical vibration intensities across the center in the schematic drawing.

The function of Archimedean spiral curve is $\rho = k\theta$. In order to meet the phase matching condition, the gap distance between two adjacent spiral lines should be equal to the integral times of the wavelength of the SAW, hence setting to be one wavelength in Figure S11. The radius of the inner element is set to be 2 μm, considering the Rayleigh Wave velocity at 9.25 GHz as an approximation. We then obtain the spiral curve to spin outward counterclockwise for a wavelength after the θ increases 2π.

For our case when all the nanodisks can launch hypersonic waves in phase, the location differences between every single antenna to the center point can intrinsically lead to the curly phase profile as we move from the antennas towards the center, thus forming a spinning hypersonic wave with orbital angular momentum defined by the designed distribution of unidirectional nanoantennas.

Here we provide the amplitude and phase distributions in Figure S12 from which we can clearly observe the azimuthally spinning of hypersonic OAMs. We also submit an animation of the GaP disk clusters vibrating at 8.6 GHz where the acoustic wave with $m = -1$ orbital angular momentum can be identified.

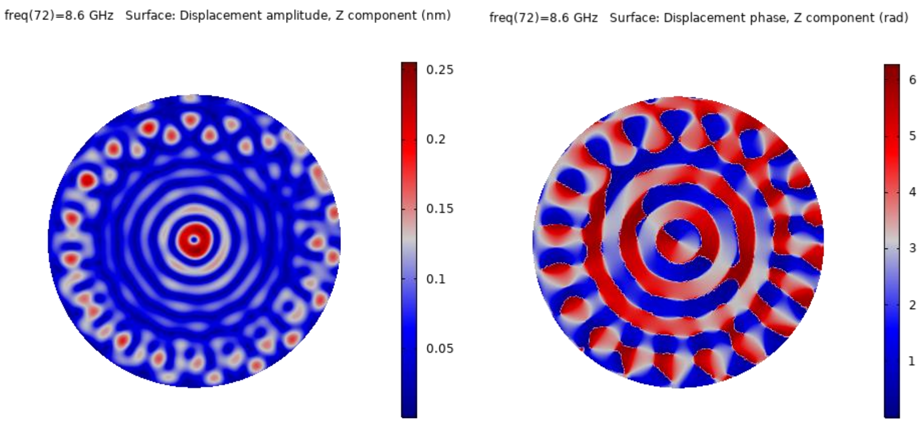

Figure S12. The amplitude and phase distributions of SAWs at 8.6 GHz. The radius of displayed circular area is 1.6 μm.